

Phase Shifter Operation of the Azimuthally Magnetized Coaxial Ferrite Waveguide

M.N. GEORGIEVA-GROSSE^a AND G.N. GEORGIEV^b

^a2, Tcherny Vrikh Str., BG-5138 Polikraishte, Bulgaria

^bFaculty of Mathematics and Informatics, University of Veliko Tirnovo "St. St. Cyril and Methodius"
BG-5000 Veliko Tirnovo, Bulgaria

(Received May 5, 2012)

The terms for operation of the coaxial waveguide, entirely filled with azimuthally magnetized latching ferrite, as a digital nonreciprocal phase shifter for the normal TE_{01} mode, are found. They are classified as physical, mathematical and functional ones. The physical prerequisites are drawn from the phase curves of the structure and specify the boundaries of the interval in which it produces differential phase shift for a given numerical equivalent of the modulus of off-diagonal ferrite permeability tensor element. The mathematical condition brings the parameters of configuration together with certain roots of its characteristic equation, derived in terms of complex Kummer and Tricomi confluent hypergeometric functions and with the related to them positive real $L_2(c, \rho, n)$ numbers ($c = 3$, $0 < \rho < 1$, $n = 1$). The functional criteria determine the borders of the domain of phase shifter operation of the geometry. These are functions, defined for a fixed central conductor thickness which express in normalized form the impact of the guide radius on the phase shift at the cut-off frequencies and at the envelopes, denoting the termination of the phase curves for negative ferrite magnetization from the side of higher frequencies. The same are reckoned, employing iterative methods, consisting in a repeated numerical solution of the equation mentioned, followed by a computation of the guide radius and phase constant of the wave and are plotted graphically. The influence of the parameters of transmission line on the area referred to is analyzed.

PACS: 02.60.Lj, 02.90.+p, 41.20.-q, 41.20.Jb, 85.70.Ge

1. Introduction

It is thought that the circular waveguides, comprising coaxially positioned cylindrical or toroidal inserts of azimuthally magnetized ferrite that support normal TE_{01} mode, are natural microwave structures for digital nonreciprocal phase shifters [1–35]. This is due to their ability to afford differential phase shift when latching the magnetization between its two stable states and to their symmetry by reason of which the electromagnetic wave interacts with the entire body of the anisotropic medium. The devices in question could be employed in the design of electronically scanned antenna arrays [36–40]. Such is e.g. the Kashin and Safonov monopulse transmit-receive phased array with polarization of targets in the main beam [40]. As an antenna element for the X and C bands a composition has been proposed, constructed of a phase shifter of the type referred to and of axially symmetric transmitters which could be manufactured of the same material. The magnetizing conductor passes along the centre-line of the setup and has two shoulders, serving like current inputs. Symmetrizing wires are placed in their neighbourhood, providing independence of the propagation conditions of the wave inside the phase shifter of its polarization. Steps are taken to match the wires inhomogeneity. This mechanism enables a phasing of the elements of the array with the help of one and the same control program for whatever polarization. It is nonreciprocal and needs rephrasing in changing the transmit and receive regimes of the antenna.

In this investigation three kinds of criteria for phase shifter operation of a coaxial ferrite waveguide with azi-

muthal magnetization which sustains normal TE_{01} mode, are established. With that end in view, the phase curves of the transmission line, some roots of its characteristic equation, written by complex confluent hypergeometric functions and the bound up with them positive real $L_2(c, \rho, n)$ numbers [30] (denoted also as $L(c, \rho, n)$ [19, 28]), are harnessed. Besides, a numerical approach, widely exploiting iterative techniques is used, too. The domain in which phase shift is produced, is depicted graphically. The influence of structure parameters on it is examined.

2. Synopsis of boundary-value problem

An infinitely long, perfectly conducting coaxial waveguide of inner and outer conductor radii r_1 and r_0 , respectively, filled entirely with latching ferrite, magnetized in azimuthal direction to remanence, is threshed out (see inset, Fig. 6), propagating normal TE_{0n} (H_r , E_θ , H_z) modes of phase constant β . A cylindrical co-ordinate system (r, ϑ, z) is accepted. The anisotropic medium possesses a Polder permeability tensor $\overset{\leftrightarrow}{\mu} = \mu_0[\mu_{ij}]$, $i, j = 1, 2, 3$, with nonzero components $\mu_{ii} = 1$ and $\mu_{13} = -\mu_{31} = -j\alpha$, $\alpha = \gamma M_r / \omega$, $-1 < \alpha < 1$ (γ — gyromagnetic ratio, M_r — ferrite remanent magnetization, ω — angular frequency of the wave) and a scalar permittivity $\varepsilon = \varepsilon_0 \varepsilon_r$ (ε_0 and μ_0 — free space permittivity and permeability, respectively). The characteristic equation of configuration [20, 25, 28]:

$$\Phi(a, c; x_0) / \Psi(a, c; x_0) = \Phi(a, c; \rho x_0) / \Psi(a, c; \rho x_0) \quad (1)$$

is represented in terms of the Kummer and Tricomi confluent hypergeometric functions $\Phi(a, c; x)$ and $\Psi(a, c; x)$,

respectively [41], in which $a = 1.5 - jk$, $c = 3$, $x_0 = jz_0$, $k = \alpha\bar{\beta}/(2\bar{\beta}_2)$, $-\infty < k < +\infty$, $\bar{\beta}_2 = (1 - \alpha^2 - \bar{\beta}^2)^{1/2}$, $z_0 = 2\bar{\beta}_2\bar{r}_0$, $z_0 > 0$, $\rho = \bar{r}_1/\bar{r}_0$, $0 < \rho < 1$ — central conductor to waveguide radius ratio. The introduction of barred (normalized) quantities: $\bar{\beta} = \beta/(\beta_0\sqrt{\varepsilon_r})$, $\bar{\beta}_2 = \beta_2/(\beta_0\sqrt{\varepsilon_r})$ ($\beta_2 = [\omega^2\varepsilon_0\mu_0\varepsilon_r(1 - \alpha^2) - \beta^2]^{1/2}$ — radial wavenumber), $\bar{r}_1 = \beta_0r_1\sqrt{\varepsilon_r}$, and $\bar{r}_0 = \beta_0r_0\sqrt{\varepsilon_r}$, ($\beta_0 = \omega\sqrt{\varepsilon_0\mu_0}$ — free space phase constant) permits to obtain general results, holding for all admissible values of parameters and all frequency bands in which transmission may be realized. If $\chi_{k,n}^{(c)}(\rho)$ ($n = 1, 2, 3, \dots$) designates the positive purely imaginary roots of Eq. (1), the same is valid in case of $\bar{\beta}_2 = \chi_{k,n}^{(c)}(\rho)/(2\bar{r}_0)$ that yields the eigenvalue spectrum of the fields explored. In what follows normal TE_{01} mode ($n = 1$) is examined solely.

3. Some features of the coaxial waveguide with azimuthally magnetized ferrite

3.1. Main points

The analysis of the phase curves of geometry under study [19], parts of which are reproduced in Figs. 1–3, discloses its nonreciprocal character which is manifested in the following [28]:

i) For all allowable numerical equivalents of the magnitude of off-diagonal ferrite permeability tensor element $|\alpha|$ there are values of the normalized guide radius \bar{r}_0 for which propagation may take place with two different phase constants $\bar{\beta}_+$ and $\bar{\beta}_-$, corresponding to positive and negative magnetization. Without exception it holds: $\bar{\beta}_- > \bar{\beta}_+$. Accordingly, the $\bar{\beta}_-(\bar{r}_0)$ — characteristics (drawn by dashed lines) are situated above the $\bar{\beta}_+(\bar{r}_0)$ — ones (plotted by solid curves), (cf. Figs. 1–3 and Fig. 1 in [19]). For every single pair of parameters

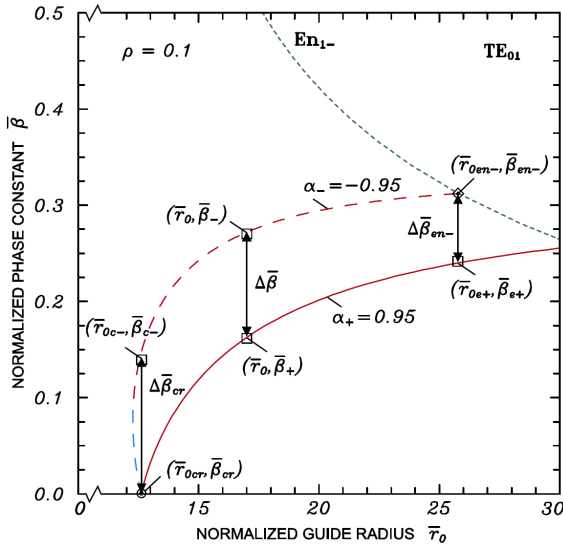


Fig. 1. Normalized phase characteristics and differential phase shift of the azimuthally magnetized coaxial ferrite waveguide for normal TE_{01} mode in case $\rho = 0.1$ and $|\alpha| = \pm 0.95$.

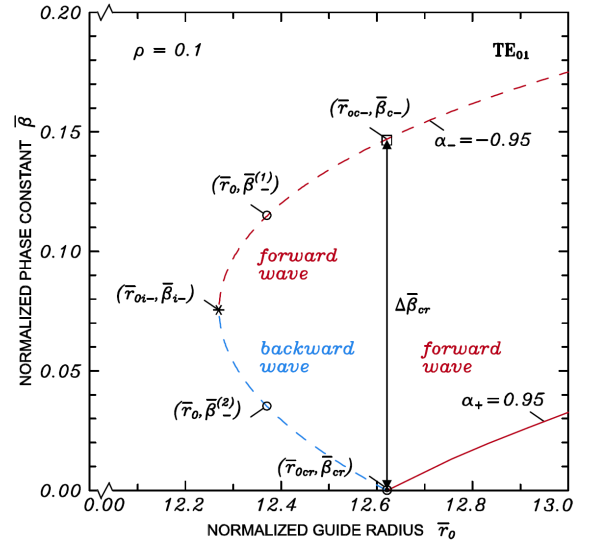


Fig. 2. Normalized phase characteristics of the azimuthally magnetized coaxial ferrite waveguide for the forward and backward normal TE_{01} mode in the vicinity of cut-off in case $\rho = 0.1$ and $|\alpha| = \pm 0.95$.

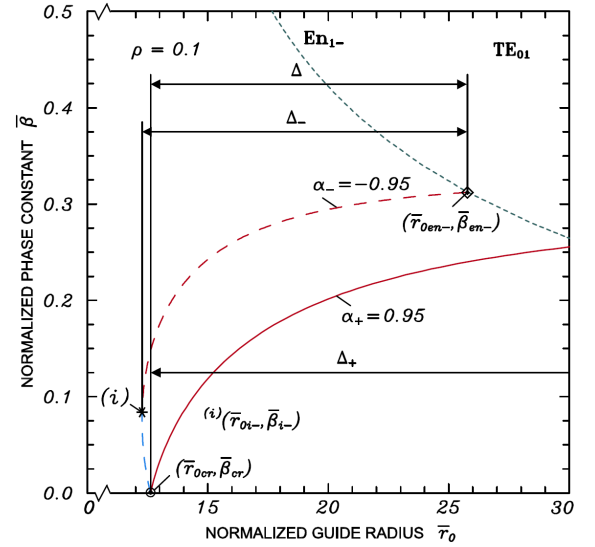


Fig. 3. Graphical illustration of the physical criterion for phase shifter operation of the azimuthally magnetized coaxial ferrite waveguide for normal TE_{01} mode in case $\rho = 0.1$ and $|\alpha| = \pm 0.95$.

$\{\bar{r}_0, |\alpha|\}$, differential phase shift $\Delta\bar{\beta} = \bar{\beta}_- - \bar{\beta}_+$ may be obtained. The quantity $\Delta\bar{\beta}$ is always positive (see Fig. 1);

ii) All $\bar{\beta}_-(\bar{r}_0)$ — curves are finite and the $\bar{\beta}_+(\bar{r}_0)$ — ones — infinite. The couple of $\bar{\beta}_-(\bar{r}_0)$ and $\bar{\beta}_+(\bar{r}_0)$ — characteristics for the same $|\alpha|$ originates in the cut-off frequency (bifurcation) point $(\bar{r}_{0cr}, \bar{\beta}_{cr})$ at the horizontal axis of phase portrait, denoted by a circle (cf. Figs. 1–3 and Fig. 1 in [19]). A special En_{1-} — envelope (depicted by a green dotted line) exists, restricting the $\bar{\beta}_-(\bar{r}_0)$ — curves from the side of higher frequencies. The $\bar{\beta}_+(\bar{r}_0)$ — characteristics are unlimited from above (see Figs. 1 and 3, and Fig. 1 in [19]);

iii) The $\bar{\beta}_-(\bar{r}_0)$ - curves have a bulge (area of double-valuedness) below cut-off. The leftmost (inversion) point $(\bar{r}_{0i-}, \bar{\beta}_{i-})$ (shown by a star) denotes the lowest frequency for which propagation may take place for $\alpha_- < 0$ (cf. Fig. 2). For the same \bar{r}_0 from the interval $(\bar{r}_{0i-}, \bar{r}_{0cr})$ the structure may guide a forward and a backward wave (whose characteristics are portrayed by red and blue dashed lines, respectively) with two different phase constants $\bar{\beta}_-^{(1)}$ and $\bar{\beta}_-^{(2)}$ ($\bar{\beta}_-^{(1)} > \bar{\beta}_-^{(2)}$), respectively on condition that $\alpha_- < 0$. No transmission is possible in this area provided $\alpha_+ > 0$ (see Fig. 2);

iv) A magnetically controlled cut-off is observed. If $\bar{r}_0 = \bar{r}_{0cr}$, the propagation stops when $\alpha_+ > 0$ and $\bar{\beta}_{cr+} = 0$ ($k_{cr+} = 0$). In case $\alpha_- < 0$, however, for the same \bar{r}_0 , ($\bar{r}_0 = \bar{r}_{0c-} \equiv \bar{r}_{0cr}$) two waves of different phase constants may be excited. The first of them is in cut-off regime and for it $\bar{\beta}_{cr-} = 0$ ($k_{cr-} = 0$, $\bar{\beta}_{cr-} \equiv \bar{\beta}_{cr-}^{(2)}$). The second wave is in transmission state with constant $\bar{\beta}_{c-} \neq 0$ ($k_{c-} \neq 0$, $k_{c-} < k_{cr-}$, $\bar{\beta}_{c-} \equiv \bar{\beta}_{c-}^{(1)}$) (cf. Fig. 2).

3.2. Some important formulae

i) The phase curves are calculated from [25, 28]:

$$\bar{r}_0 = \left(k\chi_{k,n}^{(c)}(\rho)/\alpha \right) \left\{ \left[1 + (\alpha/(2k))^2 \right] / (1 - \alpha^2) \right\}^{1/2}, \quad (2)$$

$$\bar{\beta} = \left\{ (1 - \alpha^2) / \left[1 + (\alpha/(2k))^2 \right] \right\}^{1/2}. \quad (3)$$

ii) The critical guide radius is determined by the expression [25, 28]:

$$\bar{r}_{0cr} = \chi_{0,n}^{(c)}(\rho) / \left(2\sqrt{1 - \alpha_{cr}^2} \right). \quad (4)$$

iii) The equation $\bar{\beta}_{en-} = \bar{\beta}_{en-}(\bar{r}_{0en-})$ of the envelope, written in parametric form, is [19, 25, 28]:

$$\bar{r}_{0en-} = L_2(c, \rho, n) / \left[|\alpha_{en-}| (1 - \alpha_{en-}^2)^{1/2} \right], \quad (5)$$

$$\bar{\beta}_{en-} = (1 - \alpha_{en-}^2)^{1/2}, \quad (6)$$

where $L_2(c, \rho, n)$ are certain positive real numbers [30] and $\alpha_{en-} < 0$ is a parameter. Assuming $\rho = 0.1$ and 0.5 , it is found out that: $\chi_{0,n}^{(c)}(\rho) = \mathbf{7.88188\ 32204}$ and $\mathbf{12.78631\ 35232}$, and $L_2(c, \rho, n) = \mathbf{7.65009}$ and $\mathbf{30.06288}$ ($c = 3, n = 1$). The following subscripts are used: (i) “+” (“-”) for the quantities, answering to the positive (negative) magnetization; (ii) “cr” (“c-”) for the ones, relating to cut-off (to transmission state for $\alpha_- < 0$, linked with the cut-off, cf. item (iv) in Sect. 3.1); (iii) “en-” (“e+”) for those, describing the envelope (the point from the $\bar{\beta}_+(\bar{r}_0)$ - curve for certain $|\alpha|$ of abscissa equal to that of the end point of the $\bar{\beta}_-(\bar{r}_0)$ - one for the same $|\alpha|$ at the envelope); see Figs. 1, 2.

4. Physical prerequisites for phase shifter operation

Bearing in mind the abovesaid, it might be concluded that for any ρ and fixed $|\alpha|$ [28]:

i) At positive (negative) ferrite magnetization normal TE_{01} mode could be sustained in the semi-closed interval

$\Delta_+ = [\bar{r}_{0cr}, +\infty)$ (bilaterally restricted interval $\Delta_- = [\bar{r}_{0i-}, \bar{r}_{0en-}]$);

ii) For both signs of magnetization the wave may be guided in the interval $\Delta = \Delta_+ \cap \Delta_-$ ($\Delta = [\bar{r}_{0cr}, \bar{r}_{0en-}]$) of overlapping (of intersection) of Δ_+ and Δ_- ;

iii) Differential phase shift may be afforded in Δ ;

iv) For the abscissa \bar{r}_0 of the working point $(\bar{r}_0, \bar{\beta}_+)$ ($(\bar{r}_0, \bar{\beta}_-)$), lying at the curve $\bar{\beta}_+(\bar{r}_0)$ ($\bar{\beta}_-(\bar{r}_0)$) which conforms to $\alpha_+ > 0$ ($\alpha_- < 0$), it is true: $\bar{r}_0 \in \Delta_+$ ($\bar{r}_0 \in \Delta_-$).

v) For the common abscissa \bar{r}_0 of the pair of working points $(\bar{r}_0, \bar{\beta}_+)$ and $(\bar{r}_0, \bar{\beta}_-)$, situated at the curves $\bar{\beta}_+(\bar{r}_0)$ and $\bar{\beta}_-(\bar{r}_0)$, respectively for the same $|\alpha|$, it is valid: $\bar{r}_0 \in \Delta$.

Thus, the physical criterion the geometry of any ρ to behave as a phase shifter for certain $|\alpha|$, is

$$\bar{r}_{0cr} < \bar{r}_0 < \bar{r}_{0en-}. \quad (7)$$

(The above discussion is visualized in Fig. 3.)

5. Mathematical condition for phase shifter operation

The inequalities [28]:

$$\chi_{0,n}^{(c)}(\rho)/2 < \bar{r}_0 \sqrt{1 - \alpha^2} < L_2(c, \rho, n)/|\alpha| \quad (8)$$

express the mathematical criterion of the structure to work as a phase shifter. It is a direct corollary of relation (7), combined with Eqs. (4) and (5) in case $|\alpha| \equiv |\alpha_{cr}| \equiv |\alpha_{en-}|$ and specifies the sets of parameters $\{\rho, \bar{r}_0, |\alpha|\}$ for which $\Delta\bar{\beta}$ is produced. (Everywhere in Ref. [28] the symbol $L(c, \rho, n)$ stands for $L_2(c, \rho, n)$.)

6. Functional criteria for phase shifter operation

6.1. Left limiting function

Since $\bar{\beta}_{cr+} = \bar{\beta}_{cr-} = \bar{\beta}_{cr} = 0$, for the couple of points $(\bar{r}_{0c-}, \bar{\beta}_{c-})$ and $(\bar{r}_{0cr}, \bar{\beta}_{cr+})$, ($\bar{r}_{0c-} \equiv \bar{r}_{0cr}$), it is fulfilled: $\Delta\bar{\beta}_{cr} = \bar{\beta}_{c-}$ (cf. Figs. 1, 2). The function $\Delta\bar{\beta}_{cr} = \Delta\bar{\beta}_{cr}(\rho, \bar{r}_0, n)$, presented in parametric form as [28]:

$$\bar{\beta}_{c-} = \bar{\beta}_{c-}(\alpha_-, k_{c-}), \quad (9)$$

$$\bar{r}_0 = \bar{r}_0(\rho, \alpha_-, k_{c-}, n), \quad (10)$$

determines the left limit (bounded with cut-off) of the domain in which phase shift is observed, if $\bar{r}_0 \equiv \bar{r}_{0cr}$, $\bar{r}_{0cr} = \bar{r}_{0cr}(\rho, \alpha_{cr}, n)$ (see Eq. (4)) and $\alpha_- = -|\alpha_{cr}|$. Equations (9) and (10) are given explicitly by the ones (2) and (3) in which α and k are substituted by α_- and k_{c-} .

6.2. Right limiting function

At certain $|\alpha| = |\alpha_{en-}|$ for the pair of points $(\bar{r}_{0en-}, \bar{\beta}_{en-})$ and $(\bar{r}_{0e+}, \bar{\beta}_{e+})$, ($\bar{r}_{0e+} \equiv \bar{r}_{0en-}$) (see Fig. 1), it is true [28]:

$$\Delta\bar{\beta}_{en-} = \bar{\beta}_{en-} - \bar{\beta}_{e+}. \quad (11)$$

The function $\Delta\bar{\beta}_{en-} = \Delta\bar{\beta}_{en-}(\rho, \bar{r}_0, n)$, written parametrically as [28]:

$$\bar{\beta}_{en-} = \bar{\beta}_{en-}(\alpha_-), \quad (12)$$

$$\bar{\beta}_{e+} = \bar{\beta}_{e+}(\alpha_+, k_{e+}), \quad (13)$$

$$\bar{r}_0 = \bar{r}_0(\rho, \alpha_+, k_{e+}, n), \quad (14)$$

specifies the right limit (connected with the envelope) of the area in which $\Delta\bar{\beta}$ is available in case $\bar{r}_0 \equiv \bar{r}_{0en-}$, $\bar{r}_{0en-} = \bar{r}_{0en-}(\rho, \alpha_{en-}, n)$ (see Eq. (5)) and $\alpha_- \equiv -\alpha_+ \equiv -|\alpha_{en-}|$. Equations (13) and (14) are equivalent to the ones (2) and (3) with α_+ and k_{e+} , replacing α and k , and Eq. (12) represents the one (6), respectively in it α_- stands for α_{en-} ($n = 1$ for TE_{01} mode).

7. Iterative method for tracing the left limit of the domain of phase shifter operation

7.1. Description of the method

First, values of the ratio ρ^{ch} and of the off-diagonal tensor element $|\alpha^{ch}|$ are singled out and the relevant one of the critical radius \bar{r}_{0cr}^{comp} is counted from formula (4). Next, for an arbitrarily picked out negative numerical equivalent k_-^{ch} of the imaginary part k of the parameter a of the confluent functions, the positive purely imaginary roots $\chi_{k_-^{ch}, n}^{(c)comp}(\rho^{ch})$ of Eq. (1) in x_0 (in z_0) are determined ($n = 1, 2, 3, \dots$). Then, the numbers, answering to α_-^{ch} , k_-^{ch} and $\chi_{k_-^{ch}, n}^{(c)comp}(\rho^{ch})$ are put in expressions (2), (3). After that k_-^{ch} is changed and the scheme is hammered away, until an interval of values $\Delta k_{c-}^{ch} = [k_{c-,left}^{ch}, k_{c-,right}^{ch}]$, ($k_{c-,left}^{ch} < k_{c-,right}^{ch}$) is specified, such that \bar{r}_{0cr}^{comp} lies in the pertinent one $\Delta \bar{r}_{0c-}^{comp} = [\bar{r}_{0c-,left}^{comp}, \bar{r}_{0c-,right}^{comp}]$, ($\bar{r}_{0c-,left}^{comp} < \bar{r}_{0c-,right}^{comp}$). Then Δk_{c-}^{ch} is divided into m^{ch} parts and that of them is considered for which the relevant interval for \bar{r}_{0c-}^{comp} contains \bar{r}_{0cr}^{comp} . The procedure goes on, until it becomes true: $|\bar{r}_{0cr}^{comp} - \bar{r}_{0c-}^{comp}| < \varepsilon^{ch}$, ε^{ch} — the prescribed accuracy. The value of $\bar{\beta}_{c-}^{comp}$, corresponding to the last iteration is taken as that, searched for. Afterwards, $|\alpha^{ch}|$ is altered and what has been described is repeated. Finally, a new ρ^{ch} is accepted and the calculations are done again. The chosen (computed) quantities are marked by a superscript “ ch ” (“ $comp$ ”).

7.2. Numerical example

Let $\rho^{ch} = 0.1$ and $|\alpha^{ch}| = 0.1$. Accordingly, it is found that: $\bar{r}_{0cr}^{comp} = \mathbf{3.96079\ 53460}$. Let now $k_-^{ch} = -0.1$ be an arbitrary chosen negative value of the parameter k . On doing for it the relevant computations, it is obtained: $\chi_{k_-^{ch}, n}^{(c)comp}(\rho^{ch}) = 7.50329\ 93839$, $\bar{r}_{0c-}^{comp} = 8.43120\ 56878$ and $\bar{\beta}_{c-}^{comp} = 0.88994\ 38185$. Due to the fact that $\bar{r}_{0c-}^{comp} \neq \bar{r}_{0cr}^{comp}$ ($\bar{r}_{0c-}^{comp} > \bar{r}_{0cr}^{comp}$), the process should continue. Taking $k_-^{ch} = -0.2$, yields: $\chi_{k_-^{ch}, n}^{(c)comp}(\rho^{ch}) = 7.14087\ 84197$, $\bar{r}_{0c-}^{comp} = 14.79546\ 11718$ and $\bar{\beta}_{c-}^{comp} = 0.96527\ 95998$, respectively. In this case \bar{r}_{0c-}^{comp} is even larger than in the previous one. Hence, the value of k_{c-} sought is smaller than the ones, already used. For $k_-^{ch} = -\mathbf{0.0024}$

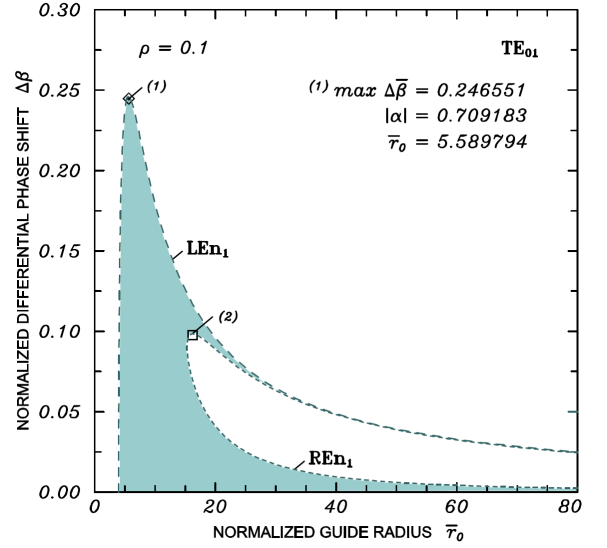


Fig. 4. Domain of phase shifter operation of the azimuthally magnetized coaxial ferrite waveguide for normal TE_{01} mode, in case $\rho = 0.1$ for the intervals $\bar{r}_0 = \langle 0 \div 80 \rangle$ and $\Delta\bar{\beta} = \langle 0 \div 0.30 \rangle$.

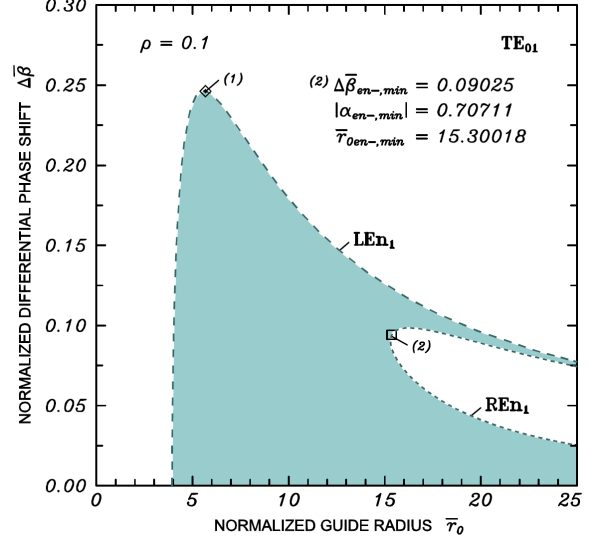


Fig. 5. Domain of phase shifter operation of the azimuthally magnetized coaxial ferrite waveguide for normal TE_{01} mode in case $\rho = 0.1$ for the intervals $\bar{r}_0 = \langle 0 \div 25 \rangle$ and $\Delta\bar{\beta} = \langle 0 \div 0.30 \rangle$.

and $k_-^{ch} = -\mathbf{0.0025}$ it is reckoned: $\chi_{k_-^{ch}, n}^{(c)comp}(\rho^{ch}) = \mathbf{7.87261\ 37226}$, $\bar{r}_{0c-}^{comp} = \mathbf{3.96069\ 20961}$, $\bar{\beta}_{c-}^{comp} = \mathbf{0.04770\ 44730}$ and $\chi_{k_-^{ch}, n}^{(c)comp}(\rho^{ch}) = \mathbf{7.87222\ 76858}$, $\bar{r}_{0c-}^{comp} = \mathbf{3.96088\ 50996}$, $\bar{\beta}_{c-}^{comp} = \mathbf{0.04968\ 73015}$, respectively. Thus, an interval $\Delta \bar{r}_{0c-}^{comp}$ has been found, containing \bar{r}_{0cr}^{comp} , respectively ones for k_-^{ch} and $\bar{\beta}_{c-}^{comp}$ have been determined, involving the values sought.

Let $m^{ch} = 10$ and the interval for k_-^{ch} in question be divided into 10 parts. Since \bar{r}_{0cr}^{comp} lies between the values of \bar{r}_{0c-}^{comp} , answering to $k_-^{ch} = -\mathbf{0.00245}$ and

$k_{c-}^{ch} = -0.00246$, these are admitted as left and right-hand sides of the subsequent interval to be treated. The relevant numerical equivalents of $\bar{r}_{0c-}^{\text{comp}}$ and $\bar{\beta}_{c-}^{\text{comp}}$ are accepted as first approximations to the quantities looked for (cf. Table I). In a similar manner, it is ascertained that the following intervals for k_{c-}^{ch} to be threshed out should be: $[-0.002455, -0.002454]$, $[-0.0024546, -0.0024545]$, etc. Table I contains the results of computations at the both limits of pertinent intervals for the first 6 iterations in case $\rho^{ch} = 0.1$ and

$\rho^{ch} = 0.5$, assuming $|\alpha^{ch}| = 0.1$. Data, corresponding to the arbitrary change of k_{c-}^{ch} , are not included. Table II yields the upshots of numerical investigation for the same ρ^{ch} and $|\alpha^{ch}| = 0.1$ (0.2) 0.9. Besides, its fifth and second columns represent the function $\Delta\bar{\beta}_{cr} = \Delta\bar{\beta}_{cr}(\rho, \bar{r}_0, n)$ (cf. Sect. 6.1) numerically for discrete values of parameters. Using the outcomes of numerical study, this function is plotted graphically in Figs. 4–7 by dashed green LEn_1 – lines in the intervals $\bar{r}_0 = \langle 0 \div 80 \rangle$ and $\langle 0 \div 25 \rangle$ for the aforesaid numerical equivalents of ρ and n .

TABLE I

Numerical values of the quantities k_{c-}^{ch} ; $\chi_{k_{c-}^{ch},1}^{(c)\text{comp}}(\rho^{ch})$, ($c = 3$); $\bar{\beta}_{c-}^{\text{comp}}$ for normal TE_{01} mode in case $|\alpha^{ch}| = 0.1$ and $m^{ch} = 10$ as a function of the number of iteration N , assuming $\rho^{ch} = 0.1$, $\bar{r}_{0cr}^{\text{comp}} = \mathbf{3.96079\ 53460}$ and $\rho^{ch} = 0.5$, $\bar{r}_{0cr}^{\text{comp}} = \mathbf{6.42536\ 43043}$.

| N | k_{c-}^{ch} | $\chi_{k_{c-}^{ch},1}^{(c)\text{comp}}(\rho^{ch})$ | $\bar{r}_{0c-}^{\text{comp}}$ | $\bar{\beta}_{c-}^{\text{comp}}$ | N | k_{c-}^{ch} | $\chi_{k_{c-}^{ch},1}^{(c)\text{comp}}(\rho^{ch})$ | $\bar{r}_{0c-}^{\text{comp}}$ | $\bar{\beta}_{c-}^{\text{comp}}$ |
|-------------------|---------------|--|-------------------------------|----------------------------------|-----|----------------|--|-------------------------------|----------------------------------|
| $\rho^{ch} = 0.1$ | | | | | | | | | |
| 1 | -0.00246 | 7.87238 20987 | 3.96080 60098 | 0.04889 42400 | 4 | -0.00245 451 | 7.87240 32920 | 3.96079 53512 | 0.04878 53850 |
| | -0.00245 | 7.87242 07023 | 3.96078 66307 | 0.04869 59600 | | -0.00245 450 | 7.87240 33306 | 3.96079 53318 | 0.04878 51867 |
| 2 | -0.00245 5 | 7.87240 14005 | 3.96079 63006 | 0.04879 51007 | 5 | -0.00245 4508 | 7.87240 32998 | 3.96079 53473 | 0.04878 53453 |
| | -0.00245 4 | 7.87240 52608 | 3.96079 43635 | 0.04877 52727 | | -0.00245 4507 | 7.87240 33036 | 3.96079 53454 | 0.04878 53255 |
| 3 | -0.00245 46 | 7.87240 29446 | 3.96079 55256 | 0.04878 71695 | 6 | -0.00245 45074 | 7.87240 33021 | 3.96079 53462 | 0.04878 53334 |
| | -0.00245 45 | 7.87240 33306 | 3.96079 53318 | 0.04878 51867 | | -0.00245 45073 | 7.87240 33025 | 3.96079 53460 | 0.04878 53314 |
| $\rho^{ch} = 0.5$ | | | | | | | | | |
| 1 | -0.00106 | 12.78344 66774 | 6.42536 70820 | 0.02108 89951 | 4 | -0.00105 796 | 12.78345 21941 | 6.42536 43051 | 0.02104 84269 |
| | -0.00105 | 12.78347 37202 | 6.42535 35716 | 0.02089 01304 | | -0.00105 795 | 12.78345 22212 | 6.42536 42915 | 0.02104 82280 |
| 2 | -0.00105 8 | 12.78345 20859 | 6.42536 43594 | 0.02104 92223 | 5 | -0.00105 7960 | 12.78345 21941 | 6.42536 43051 | 0.02104 84269 |
| | -0.00105 7 | 12.78345 47902 | 6.42536 30019 | 0.02102 93359 | | -0.00105 7959 | 12.78345 21968 | 6.42536 43037 | 0.02104 84070 |
| 3 | -0.00105 80 | 12.78345 20859 | 6.42536 43594 | 0.02104 92223 | 6 | -0.00105 79595 | 12.78345 21955 | 6.42536 43044 | 0.02104 84169 |
| | -0.00105 79 | 12.78345 23564 | 6.42536 42235 | 0.02104 72337 | | -0.00105 79594 | 12.78345 21957 | 6.42536 43042 | 0.02104 84150 |

TABLE II

Numerical values of the quantities $\bar{r}_{0c-}^{\text{comp}}$, k_{c-}^{comp} , $\chi_{k_{c-}^{\text{comp}},1}^{(c)\text{comp}}(\rho^{ch})$, $\bar{\beta}_{c-}^{\text{comp}}$ for normal TE_{01} mode for $|\alpha^{ch}| = 0.1(0.2)0.9$ and $\rho^{ch} = 0.1$ and $\rho^{ch} = 0.5$, ($c = 3$).

| $ \alpha^{ch} $ | $\bar{r}_{0c-}^{\text{comp}}$ | k_{c-}^{comp} | $\chi_{k_{c-}^{\text{comp}},1}^{(c)\text{comp}}(\rho^{ch})$ | $\bar{\beta}_{c-}^{\text{comp}}$ |
|-------------------|-------------------------------|------------------------|---|----------------------------------|
| $\rho^{ch} = 0.1$ | | | | |
| 0.1 | 3.96079 53460 | -0.00245 45073 | 7.87240 33024 | 0.04878 53316 |
| 0.3 | 4.13122 93324 | -0.02232 73862 | 7.79599 19919 | 0.14044 57848 |
| 0.5 | 4.55060 73990 | -0.06340 30242 | 7.64001 24956 | 0.21289 46115 |
| 0.7 | 5.51842 20491 | -0.12870 14588 | 7.39759 54837 | 0.24646 83154 |
| 0.9 | 9.04114 01165 | -0.22387 61940 | 7.05680 58873 | 0.19415 58038 |
| $\rho^{ch} = 0.5$ | | | | |
| 0.1 | 6.42536 43043 | -0.00105 79595 | 12.78345 21956 | 0.02104 84160 |
| 0.3 | 6.70184 92920 | -0.00953 89116 | 12.76053 75130 | 0.06054 13195 |
| 0.5 | 7.38218 15546 | -0.02659 37468 | 12.71457 90959 | 0.09160 66057 |
| 0.7 | 8.95221 00874 | -0.05241 21854 | 12.64531 53139 | 0.10576 29670 |
| 0.9 | 14.66690 75022 | -0.08728 87917 | 12.55234 46762 | 0.08300 46218 |

7.3. Maximum value of the normalized differential phase shift

Analyzing the numerical results obtained, it might be concluded that $\Delta\bar{\beta}_{cr}$ is a smooth continuous convex function of $|\alpha|$ (of $\bar{r}_0 \equiv \bar{r}_{0cr}$), possessing a maximum which is attained in both cases in the vicinity of point $|\alpha| = 0.7$ (cf. Table II). Its exact location is found by means of an iterative procedure, consisting in a successive computa-

tion of $\Delta\bar{\beta}_{cr}$ for varying $|\alpha|$ around the latter. Performing a number of iterations, the next is calculated for $|\alpha^{\text{comp}}|$, $\bar{r}_{0c-}^{\text{comp}}$, k_{c-}^{comp} , $\chi_{k_{c-}^{\text{comp}},1}^{(c)\text{comp}}(\rho^{ch})$ and $\bar{\beta}_{c-}^{\text{comp}}$ when $\rho^{ch} = 0.1$ and 0.5, respectively: **0.709183**, **5.58979** 42553 16039, **-0.13235** 98055 22100, **7.38421** 88422 72688, **0.24655** **08703** **95035**; **0.707148**, **9.04181** 60967 85339, **-0.05350** 05006 62200, **12.64240** 38742 22261, **0.10578** **43737** **58764**.

TABLE III

Numerical values of the quantities k_{e+}^{ch} ; $\chi_{k_{e+}^{ch},1}^{(c)\text{comp}}(\rho^{ch})$, ($c = 3$); $\bar{r}_{0e+}^{\text{comp}}$; $\bar{\beta}_{e+}^{\text{comp}}$ for normal TE_{01} mode in case $|\alpha^{ch}| = 0.1$ and $m^{ch} = 10$ as a function of the number of iteration N , assuming $\rho^{ch} = 0.1$, $\bar{r}_{0en-}^{\text{comp}} = \mathbf{76.88630}$ and $\rho^{ch} = 0.5$, $\bar{r}_{0en-}^{\text{comp}} = \mathbf{302.14331}$.

| N | k_{e+}^{ch} | $\chi_{k_{e+}^{ch},1}^{(c)\text{comp}}(\rho^{ch})$ | $\bar{r}_{0e+}^{\text{comp}}$ | $\bar{\beta}_{e+}^{\text{comp}}$ | N | k_{e+}^{ch} | $\chi_{k_{e+}^{ch},1}^{(c)\text{comp}}(\rho^{ch})$ | $\bar{r}_{0e+}^{\text{comp}}$ | $\bar{\beta}_{e+}^{\text{comp}}$ |
|-------------------|--------------------------------------|--|--|--|-----|--|--|--|--|
| $\rho^{ch} = 0.1$ | | | | | | | | | |
| 1 | 0.700 0.701 | 10.89669 40203 10.90133 70267 | 76.85644 21512 76.99847 46765 | 0.99245 88754 0.99246 60570 | 4 | 0.70021 0 0.70021 1 | 10.89766 89980 10.89767 36408 | 76.88626 08155 76.88640 28195 | 0.99246 03860 0.99246 03932 |
| 2 | 0.7002 0.7003 | 10.89762 25698 10.89808 68543 | 76.88484 07807 76.89904 15721 | 0.99246 03141 0.99246 10331 | 5 | 0.70021 02 0.70021 03 | 10.89766 99265 10.89767 03908 | 76.88628 92163 76.88630 34167 | 0.99246 03875 0.99246 03882 |
| 3 | 0.70021 0.70022 | 10.89766 89980 10.89771 54262 | 76.88626 08155 76.88768 08602 | 0.99246 03860 0.99246 04580 | 6 | 0.70021 027 0.70021 028 | 10.89767 02515 10.89767 02980 | 76.88629 91566 76.88630 05766 | 0.99246 03880 0.99246 03881 |
| $\rho^{ch} = 0.5$ | | | | | | | | | |
| 1 | 1.6662 1.6663 | 18.03345 54248 18.03381 11588 | 302.12310 36994 302.14717 99901 | 0.99453 97443 0.99453 97980 | 4 | 1.66628 39 1.66628 40 | 18.03375 38863 18.03375 42412 | 302.14330 36706 302.14332 77316 | 0.99453 97893 0.99453 97894 |
| 2 | 1.66628 1.66629 | 18.03374 00122 18.03377 55855 | 302.14236 46773 302.14477 23304 | 0.99453 97872 0.99453 97926 | 5 | 1.66628 392 1.66628 393 | 18.03375 39577 18.03375 39959 | 302.14330 84893 302.14331 09409 | 0.99453 97893 0.99453 97893 |
| 3 | 1.66628 3 1.66628 4 | 18.03375 06850 18.03375 42415 | 302.14308 69859 302.14332 77380 | 0.99453 97888 0.99453 97894 | 6 | 1.66628 3926 1.66628 3927 | 18.03375 39759 18.03375 39841 | 302.14330 98811 302.14331 01992 | 0.99453 97893 0.99453 97893 |

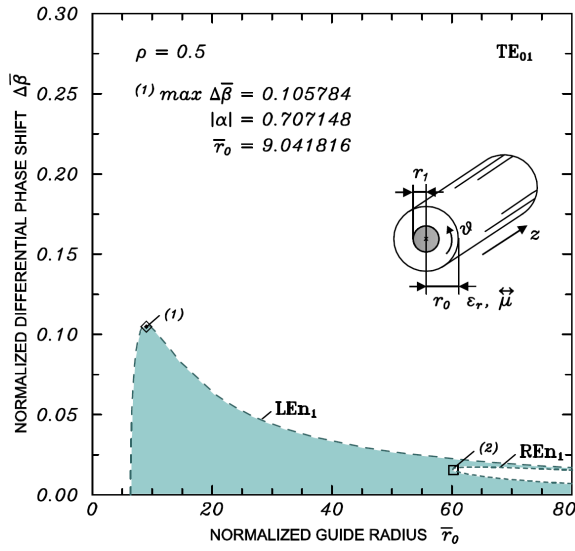


Fig. 6. Domain of phase shifter operation of the azimuthally magnetized coaxial ferrite waveguide for normal TE_{01} mode in case $\rho = 0.5$, for the intervals $\bar{r}_0 = \langle 0 \div 80 \rangle$ and $\Delta\beta = \langle 0 \div 0.30 \rangle$.

The maximum of the LEn_1 - curve (the maximum value of $\Delta\beta$ which the relevant geometry might afford at all) is marked in Figs. 4–7 by the points (1).

8. Iterative method for tracing the right limit of the domain of phase shifter operation

8.1. Description of the method

As before, values of the parameters ρ^{ch} and $|\alpha^{ch}|$ are selected. Afterwards, the corresponding numerical equivalents of the normalized guide radius $\bar{r}_{0en-}^{\text{comp}}$ and phase constant $\bar{\beta}_{en-}^{\text{comp}}$ are reckoned from formulae (5) and (6). The $L_2(3, \rho^{ch}, 1)$ numbers are taken from Table 3 in [19]. Then the iterative scheme, described in

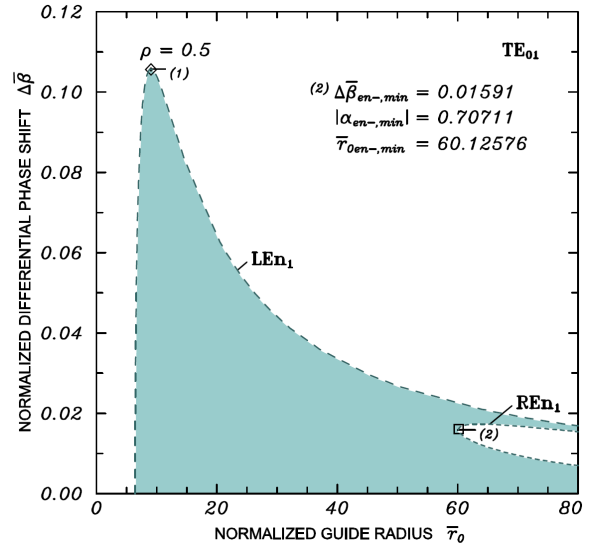


Fig. 7. Domain of phase shifter operation of the azimuthally magnetized coaxial ferrite waveguide for normal TE_{01} mode in case $\rho = 0.5$, for the intervals $\bar{r}_0 = \langle 0 \div 80 \rangle$ and $\Delta\beta = \langle 0 \div 0.12 \rangle$.

Sect. 7.1, is effectuated for positive values of parameter k_+^{ch} to get $\chi_{k_+^{ch},n}^{(c)\text{comp}}(\rho^{ch})$, respectively $\bar{r}_{0e+}^{\text{comp}}$ and $\bar{\beta}_{e+}^{\text{comp}}$ looked for. The computations go on until the inequality $|\bar{r}_{0en-}^{\text{comp}} - \bar{r}_{0e+}^{\text{comp}}| < \varepsilon^{ch}$ becomes true. The quantity $\Delta\bar{\beta}_{en-}$ is determined as a difference between $\bar{\beta}_{en-}^{\text{comp}}$ and $\bar{\beta}_{e+}^{\text{comp}}$.

8.2. Numerical example

Let like previously $\rho^{ch} = 0.1$, $|\alpha^{ch}| = 0.1$ and $m^{ch} = 10$. Formulae (5) and (6) with $L_2(3, \rho^{ch}, 1) = \mathbf{7.65009}$ yield $\bar{r}_{0en-}^{\text{comp}} = \mathbf{76.88630}$ and $\bar{\beta}_{en-}^{\text{comp}} = \mathbf{0.99499}$. For $k_+^{ch} = \mathbf{0.7}$ and $k_+^{ch} = \mathbf{0.71}$ (two arbitrary picked out positive values of k) it is obtained: $\chi_{k_+^{ch},n}^{(c)\text{comp}}(\rho^{ch}) = \mathbf{10.89669}$ 40203, $\bar{r}_{0e+}^{\text{comp}} = \mathbf{76.85644}$ 21512, $\bar{\beta}_{e+}^{\text{comp}} =$

0.99245 88754, and $\chi_{k_{e+}^{(c)comp}, n}(\rho^{ch}) = \mathbf{10.94315}$ 29996, $\bar{r}_{0e+}^{comp} = \mathbf{78.28119}$ 85959, $\beta_{e+}^{comp} = \mathbf{0.99252}$ 93390, respectively. Obviously, an interval of values for k is found such that the relevant one for \bar{r}_{0e+}^{comp} contains \bar{r}_{0en-}^{comp} . The ends of subsequent subintervals for k and the corresponding results for the quantities of interest obtained, following the described procedure, are given in Table III. The same presents also the similar data counted when $\rho^{ch} = 0.5$. The upshots for \bar{r}_{0en-}^{comp} , $\bar{\beta}_{en-}^{comp}$, k_{e+}^{comp} , $\chi_{k_{e+}^{(c)comp}, n}(\rho^{ch})$, β_{e+}^{comp} and $\Delta\bar{\beta}_{en-}$ in case $\rho^{ch} = 0.1$ and 0.5 , respectively (the first numbers) and $|\alpha^{ch}| = 0.1$ are: **0.1, 76.88630, 0.99499, 0.70021, 10.89767, 0.99246, 0.00253**; **0.5, 302.14331, 0.99499, 1.66628, 18.03375, 0.99454, 0.00045**.

The quantity \bar{r}_{0en-} has a minimum $\min \bar{r}_{0en-} = 2L_2(3, \rho, 1)$ provided $\alpha_{\min} = -1/\sqrt{2} = \mathbf{-0.70711}$ and $\bar{\beta}_{en-, \min} = |\alpha_{\min}|$ [19]. The outcomes for \bar{r}_{0en-}^{comp} , $\bar{\beta}_{en-}^{comp}$, k_{e+}^{comp} , $\chi_{k_{e+}^{(c)comp}, n}(\rho^{ch})$, $\bar{\beta}_{e+}^{comp}$, $\Delta\bar{\beta}_{en-, \min}$, respectively, with $\varepsilon^{ch} = 10^{-5}$ at this point are: (i) if $\rho^{ch} = 0.1$: **15.30018, 0.70711, 0.63093, 10.57762, 0.61686, 0.09025**; (ii) and if $\rho^{ch} = 0.5$: **60.12576, 0.70711, 1.63850, 17.93507, 0.69120, 0.01591**. The accuracy of $L_2(3, \rho, 1)$ (maximum five decimal places) [19] pre-determines the one of the upshots. (The digits in a given result, being identical with these in the final one, are distinguished by bold face type.)

In above examples the numbers, relevant to $\Delta\bar{\beta}_{en-}$ and \bar{r}_{0en-} yield the function $\Delta\bar{\beta}_{en-} = \Delta\bar{\beta}_{en-}(\rho, \bar{r}_0, n)$ (cf. Sect. 6.2) for discrete values of its parameters. The based on the numerical study dotted green REN_1 - lines in Figs. 4–7, show it graphically for $\bar{r}_0 = \langle 0 \div 80 \rangle$ and $\langle 0 \div 25 \rangle$, and the both values of ρ considered, assuming normal TE_{01} mode. The leftmost point of the REN_1 - curves is marked off by notation (2).

9. Domain of phase shifter operation

The LEN_1 - and the REN_1 - lines in Figs. 4–7 portray the limits of the domain of existence of $\Delta\bar{\beta}$ (represented by blue colour), linked with the cut-off frequencies and with the envelope of the $\beta_-(\bar{r}_0)$ - characteristics [19], respectively. As seen, for specific $\bar{r}_0 \in [\chi_{0,n}^{(c)}/2, 2L_2(c, \rho, n)]$, $\Delta\bar{\beta}$ is produced for all $|\alpha| \in [0, \alpha_{cr}]$, $\alpha_{cr} = \sqrt{1 - [\chi_{0,n}^{(c)}/(2\bar{r}_0)]^2}$ and its value varies from the \bar{r}_0 - axis to the LEN_1 - line. Provided $\bar{r}_0 \in [2L_2(c, \rho, n), +\infty]$, there are two zones below and above the REN_1 - curve in which $\Delta\bar{\beta}$ is observed, separated by one where it does not exist. In the lower (upper) zone phase shift is obtained for $|\alpha| \in [0, \alpha_2]$ ($|\alpha| \in [\alpha_1, \alpha_{cr}]$), $\alpha_{1,2} = 0.5\sqrt{1 \pm (1 - 4L_2(c, \rho, n)/\bar{r}_0)^2}$. No $\Delta\bar{\beta}$ is available, if $|\alpha| \in [\alpha_2, \alpha_1]$. The abscissa $\min \bar{r}_{0en-} = 2L_2(c, \rho, n)$ of point (2) delimits both intervals for \bar{r}_0 . Moreover, the growth of central conductor thickness lessens the maxima of LEN_1 - lines (the maximum value that $\Delta\bar{\beta}$ may attain, decreases). Simul-

taneously, the REN_1 - curve moves faster to the side of higher frequencies and the domain studied expands.

10. Conclusion

The criteria under which the azimuthally magnetized coaxial ferrite waveguide operates as a phaser shifter for normal TE_{01} mode, named as a physical, a mathematical and a functional one, are obtained. The cut-off frequency points and the peculiar envelope lines in the phase picture of configuration are used to formulate the first of them. The second condition connects the parameters of geometry with definite roots of its characteristic equation, presented by complex confluent hypergeometric functions and with the linked with them $L_2(c, \rho, n)$ numbers. The third one yields the differential phase shift afforded by the transmission line at cut-off and at the envelopes as a function of its parameters. The same is evaluated by iterative techniques, using the roots of the equation referred to. Its graphical image determines the limits of the domain of phase shifter operation of the waveguide. The potentiality of the latter as an element of a special kind of electronically scanned antenna array is also revealed.

Acknowledgments

We express our gratitude to our mother Trifonka Romanova Popnikolova and to our late father Nikola Georgiev Popnikolov for their self-denial and for their tremendous efforts to support all our undertakings.

References

- [1] D.M. Bolle, G.S. Heller, *IEEE Trans. Microwave Theory Tech.* **MTT-13**, 421 (1965). See also D.M. Bolle, N. Mohsenian, Correction, *IEEE Trans. Microwave Theory Tech.* **MTT-34**, 427 (1986).
- [2] P.J.B. Clarricoats, A.D. Olver, *Electron. Lett.* **2**, 37 (1966).
- [3] R.E. Eaves, D.M. Bolle, *Electron. Lett.* **2**, 275 (1966).
- [4] W.J. Ince, G.N. Tsandoulas, *IEEE Trans. Microwave Theory Tech.* **MTT-19**, 393 (1971).
- [5] F.J. Bernues, D.M. Bolle, *A Study of Modes in Circular Waveguide with azimuthally Magnetized Ferrite*, Div. of Engineering, Brown Univ., Providence, R.I., NSF Res. Grant NSF-GK 2351/1, Washington, D.C. 1971.
- [6] F.J. Bernues, D.M. Bolle, *Trans. Microwave Theory Tech.* **MTT-21**, 842 (1973).
- [7] O. Parriaux, Ph.D. Thesis, École Polytechnique Fédérale de Lausanne, Switzerland 1975.
- [8] O. Parriaux, F.E. Gardiol, *Wave Electronics* **1**, 363 (1976).
- [9] O. Parriaux, F.E. Gardiol, *IEEE Trans. Microwave Theory Tech.* **MTT-25**, 221 (1977).
- [10] R.S. Mueller, F.J. Rosenbaum, *J. Appl. Phys.* **48**, 2601 (1977).
- [11] S.N. Samaddar, *J. Appl. Phys.* **50**, 518 (1979).

- [12] M.E. Averbuch, in: *Proc. V. Int. Conf. on Microwave Ferrites, Vilnius (USSR)*, 1980, Vol. 4, p. 126 (in Russian).
- [13] G.A. Red'kin, A.E. Mudrov, V.A. Meshcheriakov, in Ref. [12], p. 170.
- [14] Y. Xu, J. Chen, *IEEE Trans. Magn.* **MAG-16**, 1174 (1980).
- [15] I.V. Lindell, *IEEE Trans. Microwave Theory Tech.* **MTT-30**, 1194 (1982).
- [16] A.J. Baden-Fuller, *Ferrites at Microwave Frequencies*, IEEE Electromagnetic Waves Series 23, Peter Peregrinus, London, UK 1987.
- [17] G.N. Georgiev, M.N. Georgieva-Grosse, *IEEE Antennas Wireless Propagat. Lett.* **AWPL-2**, 306 (2003).
- [18] G.N. Georgiev, M.N. Georgieva-Grosse, *J. Telecomm. Information Technol.* **JTIT-6**, 112 (2005).
- [19] G.N. Georgiev, M.N. Georgieva-Grosse, in: *Proc. XXIX URSI General Assembly, Chicago (IL)*, 2008, article ID BK.6 (120).
- [20] G.N. Georgiev, M.N. Georgieva-Grosse, in: *Proc. Joint 5th ESA Worksh. Millim. Wave Technol. Appl. & 31st ESA Antenna Workshop, ESA/ESTEC, Noordwijk (The Netherlands)*, 2009, pt. 2, p. 791.
- [21] M.N. Georgieva-Grosse, G.N. Georgiev, in: *Proc. 26th Progr. in Electromagn. Res. Symp. PIERS 2009, Moscow (Russia)*, 2009, in Abstracts, p. 612, in *PIERS Proc.*, Electromagnetics Academy, Cambridge (MA), p. 1043.
- [22] G.N. Georgiev, M.N. Georgieva-Grosse, in: *Proc. IX Kharkov Young Sci. Conf. "Radiophysics, Photonics, Electronics and Biophysics," Kharkov (Ukraine)*, 2009, p. 6.
- [23] G.N. Georgiev, M.N. Georgieva-Grosse, in: *Proc. Asia-Pacific Microwave Conf. APMC-2009, Singapore*, 2009, p. 870.
- [24] G.N. Georgiev, M.N. Georgieva-Grosse, in: *Proc. 27th Progr. Electromagn. Res. Symp. PIERS 2010, Xi'an (China)*, 2010, in Abstracts, p. 186, in *PIERS Proc.*, Electromagnetics Academy, Cambridge (MA), p. 274; *PIERS Online* **6**, 365 (2010).
- [25] M.N. Georgieva-Grosse, G.N. Georgiev, in: *Proc. 4th Europ. Conf. Antennas Propagat. EuCAP 2010, Barcelona (Spain)*, 2010, article ID P4-53, 5 pages.
- [26] M.N. Georgieva-Grosse, G.N. Georgiev, in: *Proc. 28th Progr. in Electromagn. Res. Symp. PIERS 2010, Cambridge (MA)*, in Abstracts, p. 505, in *PIERS Proc.*, Electromagnetics Academy, Cambridge (MA) 2010, p. 841.
- [27] G.N. Georgiev, M.N. Georgieva-Grosse, in: *Proc. 2010 IEEE Int. Symp. Antennas Propagat. & CNC-USNC/URSI Radio Science Meeting AP-S 2010, Toronto (ON)*, 2010, article ID 330.9.
- [28] M.N. Georgieva-Grosse, G.N. Georgiev, in: *Proc. 18th Int. Conf. Microwaves, Radar, Wireless Commun. MIKON-2010, Vilnius (Lithuania)*, Ed. B. Levitas, Geozondas, Vilnius 2010, article ID C7-3, (Focused Section).
- [29] M.N. Georgieva-Grosse, G.N. Georgiev, in: *Proc. 5th Europ. Conf. Antennas Propagat. EuCAP 2011, Rome (Italy)*, 2011, p. 1666.
- [30] G.N. Georgiev, M.N. Georgieva-Grosse, in: *Proc. Thirteenth Int. Conf. Electromagn. Adv. Applicat. ICEAA'11, Turin (Italy)*, 2011, p. 544, (Invited Paper in the Special Session "Future challenges in mathematical and computational electromagnetics and its applications", organized by G.N. Georgiev, M.N. Georgieva-Grosse).
- [31] M.N. Georgieva-Grosse, G.N. Georgiev, in: *Proc. 1st IEEE-APS Topical Conf. Antennas Propagat. Wireless Commun. IEEE APWC'11, Turin (Italy)*, 2011, p. 865, (Invited Paper in the Special Session "Advances in wireless communications and their applications," organized by M.N. Georgieva-Grosse, G.N. Georgiev).
- [32] M.N. Georgieva-Grosse, G.N. Georgiev, in: *Proc. 6th Europ. Conf. Antennas Propagat. EuCAP 2012, Prague 2012*, p. 952.
- [33] G.N. Georgiev, M.N. Georgieva-Grosse, *Telecomm. Radioeng.* **71**, 209 (2012).
- [34] G.N. Georgiev, M.N. Georgieva-Grosse, in: *Wave Propagation*, Academy Publish, Cheyenne (WY) 2012.
- [35] M.N. Georgieva-Grosse, G.N. Georgiev, in: *Proc. Fourteenth Int. Conf. Electromagn. Adv. Applicat. ICEAA'12, Cape Town (South Africa)*, 2012, article ID 496, (Invited Paper in the Special Session "Advanced applications of the mathematical and computational electromagnetics," organized by G.N. Georgiev and M.N. Georgieva-Grosse).
- [36] M.I. Andriyчук, N.N. Voitovich, P.A. Savenko, V.P. Tkachuk, in: *Numerical Methods and Algorithms*, Naukova Dumka Pub., Kiev 1993, p. 256 (in Russian).
- [37] R.C. Hansen, *Phased Array Antennas*, Wiley, New York 1998.
- [38] R.J. Mailloux, *Phased Array Antenna Handbook*, Artech House, Norwood, MA, 1st ed 1994, 2nd ed 2005.
- [39] S.P. Skobelev, *Phased Array Antennas with Optimized Element Patterns*, Artech House, Norwood, MA 2011.
- [40] V.A. Kashin, A.P. Safonov, *J. Commun. Technol. Electron.* **50**, 853 (2005) (in Russian).
- [41] F.G. Tricomi, *Confluent Hypergeometric Functions*, Gauthier-Villars, Paris, France 1960 (in French).